

Photonic band structures of ZnX (X = S, Se, Te)

U. ERDİVEN, Y. UFUKTEPE*

Physics Department, University of Cukurova 01330 Adana, Turkey

Dielectric photonic band gap materials have received broad attention due to their distinguished performance in optical devices, microwave generation and laser acceleration. We have theoretically studied photonic band structure parameters of ZnX (X = S, Se, Te). The photonic band structure calculations are performed using the MIT photonic-bands package (MPB) to calculate eigenmodes frequency domain of Maxwell's equations with periodic boundary conditions. Eigenmodes are calculated in Fourier domain. Model calculations are based on two-dimensional periodic crystal structure. The lattices consist of cylindrical rods and gaps between the rods filled with air. Single-site zinc blende lattices are considered. In order to get "gap maps" we have calculated the gaps as a function of radius of the rods. Moreover we have calculated the nature of guided modes in line defect waveguide. Our results are in good agreement with those in the literature.

(Received May 10, 2011; accepted September 15, 2011)

Keywords: Photonic band, Dielectric constant, FDTD, Group velocity, ZnS, ZnSe, ZnTe

1. Introduction

Photonic crystals (PCs) are now well acknowledged for their capability to control and manipulate the propagation of electromagnetic waves in confined space [1]. The work of Yablonovitch [2] and John [3] on such structures, often called photonic crystals, displays a range of frequency where propagation is completely forbidden. This is called the photonic band gap (PBG) and is analogous to the electronic band gap that is found in semiconductors. These dielectric materials, with complete band gaps, appear to be promising candidates for next generation optoelectronic devices and a new class of waveguiding [4-6].

ZnX (X = S, Se, Te) and related II–VI compounds, with wide and direct band gap energies, have attracted much research interest because of their excellent properties of luminescence [7-10]. Their applications in photonic crystal devices operating in the visible and near infrared (IR) region due to high indices of refraction and large band gaps make them highly transparent in the visible region [7]. It has been shown that these properties are very useful in controlling the propagation and emission of light [11]. One of the most significant features of photonic crystals is that electromagnetic waves with such frequencies within the photonic band gap (PBG) are prohibited to propagate, regardless of the polarization and propagating directions of the electromagnetic waves. The wider a PBG is, the greater the forbidden region of the frequency spectrum. Thus, the search for photonic crystals that possess wider band gaps is an important issue. According to experimental results and theoretical calculations, no complete 2D PBGs exist for a square lattice structure consisting of dielectric material cylindrical rods in the air background [3].

In this paper, we study a two-dimensional photonic crystal square lattice of the zinc-blende ZnX (X = S, Se, Te) compounds. This model is based on computing

eigenstates of Maxwell's equations for periodic dielectric systems. It should be noted that two dimensional systems exhibit most of the important characteristics of photonic crystals. Here we use two-dimensional periodic crystal structure of a square lattice of dielectric rods in air background. The rods have lattice constant a , radius $0.22a$, $0.23a$, and $0.24a$ for ZnTe, ZnSe, and ZnS respectively and dielectric constants assumed to be 5.76 for ZnS [12]; 7.12 for ZnSe; 8.7 for ZnTe [13], respectively in the spectral range from 0.3 to $1\mu\text{m}$. This structure prohibits propagation of TM light (in-plane magnetic field) in the frequency range 0.3 to 0.4 c/a . We consider two dimensional structures which are invariant in z -direction of the Cartesian coordinate system. The PCs can be fabricated easily and operated in the microwave region because lattice constant a is in the order of microwave wavelengths. Our goal is to construct novel ZnX based photonic materials to show optimal band gaps in their spectrum.

2. Computational method

The calculations were performed with the MIT Photonic Bands (MPB) Package based on finite difference time-domain (FDTD) simulations of arbitrary electromagnetic structures, which can be used to calculate band diagrams and eigenfields for the crystals [14,15]. The propagation of electromagnetic waves in photonic crystals is governed by Maxwell's equations which can be written in the following form called the Master equation:

$$\nabla \times \frac{1}{\varepsilon(\mathbf{r})} \nabla \times \mathbf{H}(\mathbf{r}) = \left(\frac{\omega}{c} \right)^2 \mathbf{H}(\mathbf{r}) \quad (1)$$

where $\varepsilon(\mathbf{r})$ is the dielectric function and c is the speed of light in vacuum, the time dependence is assumed to be $e^{-i\omega t}$. Equation (1) is in the form of eigenvalue equation where ω^2/c^2 is the eigenvalue. Since $\varepsilon(\mathbf{r})$ is periodic, we can use

the Bloch's theorem to expand both magnetic field \mathbf{H} and $\varepsilon(\mathbf{r})$ in terms of plane waves [16,17].

The time domain simulations were implemented by software MIT Electromagnetic Equation Propagation (MEEP). MEEP is a free finite-difference time-domain (FDTD) simulation software package developed to model electromagnetic systems, along with our MPB eigenmode package which is applied to computing the transmission or scattering spectra from some finite structure [18-20].

3. Results

A. Photonic Band Structure of ZnX

Fig. 1 shows TM photonic band structure for a square array of dielectric columns of ZnX. The solid lines represent wave vector from Γ to K to measure the corresponding frequencies of the propagating photon. The first TM band gaps appeared to be between the first and second bands in the frequency ranges of $(0.359-0.437) wa/2\pi c$ for ZnS, $(0.335-0.433) wa/2\pi c$ for ZnSe, $(0.310-0.423) wa/2\pi c$ for ZnTe. A complete photonic band gap (PBG) exists in the visible region for all three samples shown by a solid bar. In this frequency interval no allowed mode and the electromagnetic propagation is not possible within this gap. This means that the photon emitted from the source does not propagate but is strongly localized around the rod including the source, when the photon frequency is within the photonic band gap. This result shows well that if the spectral maximum frequency of the luminescence lies around the centre of a photonic band gap, the luminescence could be suppressed. The first calculated band width was approximately 19.4%, 25.3% and 30.6% of the central gap frequency for ZnS, ZnSe and ZnTe. There is a significant frequency shift to lower values in PBG when going from ZnS to ZnTe due to an increase of dielectric constant of the rods. We also note that a photonic band gap plot in Fig. 1 shows that the gap widens considerably as the dielectric constant is increased. Small photonic band gaps appear in after fourth TM band but these are not shown in the Fig. 1 the values of these PBG's are given in Table 1. The number of partial PBG has increased while the band widths decreased from ZnS to ZnTe. In addition to TM bands we have calculated TE-polarized modes shown in Table 1. The lowest TE bands have almost the same small band gap for all three samples, but second TE bands from ZnS and the third TE band from ZnSe disappeared.

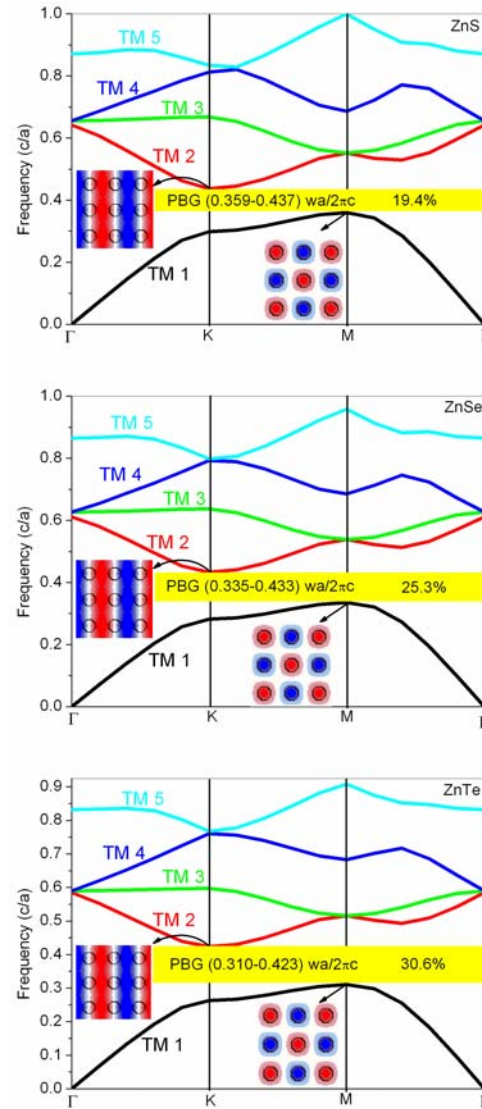


Fig. 1. The photonic band structure for a square array of dielectric columns with $r = 0.22a, 0.23a, 0.24a$ for ZnTe, ZnSe, and ZnS respectively and dielectric constants assumed to be 5.76 for ZnS; 7.12 for ZnSe; 8.7 for ZnTe. The left and middle insets show displacement fields of TM states inside a square array of dielectric columns in air. The color indicates the amplitude of the displacement field, which points in the z direction. The modes are shown at K and M points.

Table 1. Partial band gaps of ZnX (X = S, Se, Te) for TM and TE modes.

Materials	TM Band gap ($wa/2\pi c$)	TE Band gap ($wa/2\pi c$)
ZnS	TM4-TM5 (0.820-0.828)	TE4-TE5 (0.868- 0.895)
	TM6-TM7 (0.998-1.003)	
ZnSe	TM4-TM5 (0.792-0.797)	TE4-TE5 (0.853-0.873)
	TM6-TM7 (0.958-0.970)	TE5-TE6 (0.959-0.964)
ZnTe	TM4-TM5 (0.761-0.767)	TE4-TE5 (0.837-0.840)
		TE5-TE6 (0.924-0.925)
		TE7-TE8 (1.102-1.108)

Fig. 2 shows group velocity distribution of ZnX. The clear decrease in group velocity from ZnS to ZnTe can be seen in the figure. However, group velocity decreases dramatically as the mode approaches from the center of the Brillouin zone (Γ) to the (K) boundary which indicates a slow wave behavior. It is worth noting that group velocity is zero between (K) and (M) boundaries. The region between these two boundaries falls in the region of PBGs. In general, the slow wave behavior from ZnS to ZnTe was present and it might be the effect of dielectric constant.

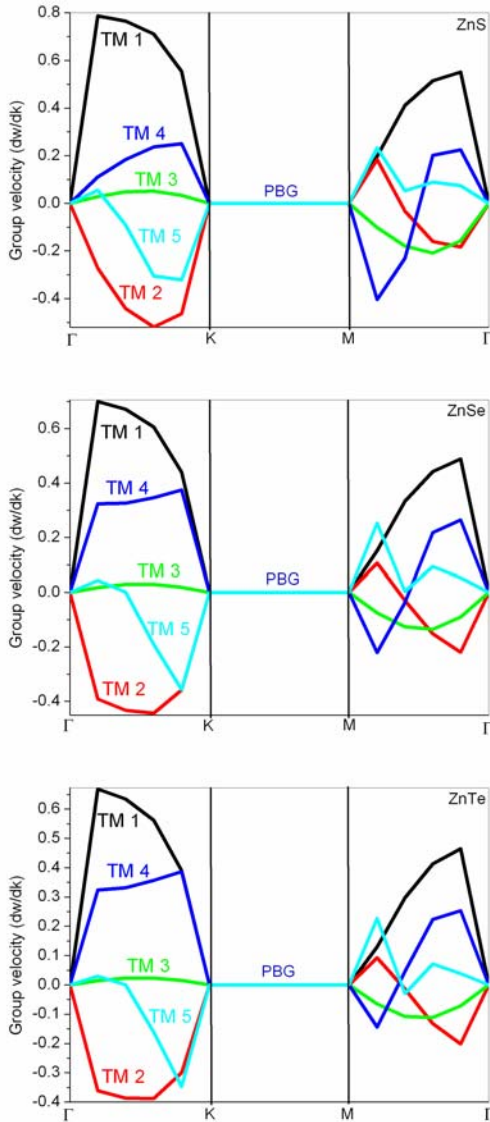


Fig. 2. Group velocity of ZnX dielectric rods shown versus wavevector.

The photonic band gap map of ZnX for the TM polarization presented in Fig. 3 it shows that the spectral width varies with the (r/a) ratio (dielectric rod diameter divided by lattice constant). The existence of a gap,

however, depends strongly on r/a ratio which clearly shows that only above a critical value of circular rod size, ($r/a \geq 0.15$ for ZnS, $r/a \geq 0.12$ for ZnSe and ZnTe) TM photonic gap can be obtained. According to the findings in Fig. 3 is that most suitable (r/a) ratio values are $0.24a$, $0.23a$, and $0.22a$ for ZnS, ZnSe and ZnTe respectively. Comparing the gap maps for the TM modes of square PC ZnX lattices, it can be concluded that ZnTe PBG map is wider. Changes in rod diameter and lattice constant can serve to fabricate different useful optical devices. The gap map could be useful in the design of ZnX rod photonic crystal light emitting devices.

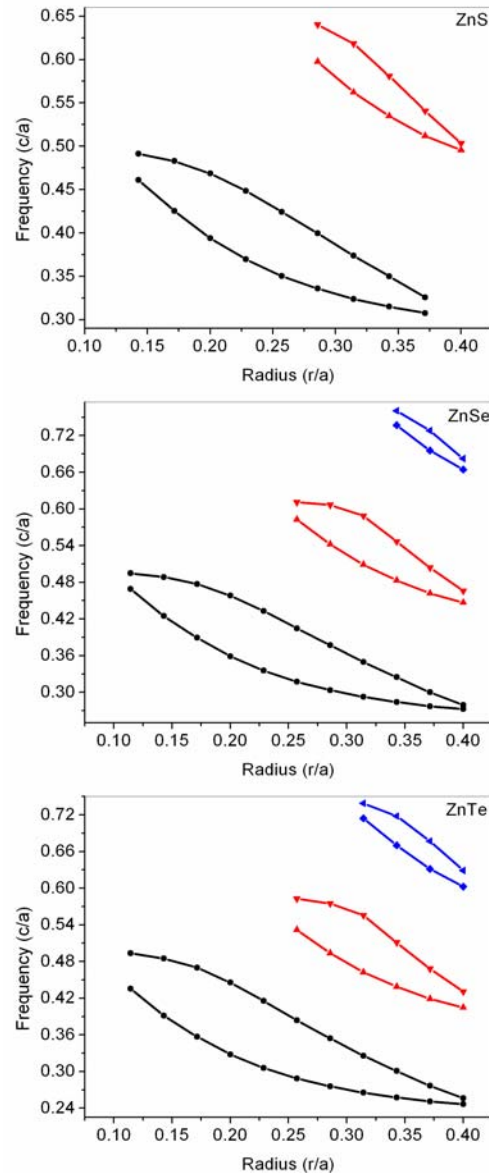


Fig. 3. Photonic gap map (normalized frequency c/a versus the ratio of r/a) for the square lattice of ZnX rods in air background for TM mode.

The complete PBG is an interesting issue for the inclusion of additional dielectric circular rods in the unit cell. In order to see the effect of the number of dielectric rods on the widths of the PBGs, we have changed the number of rods in the unit cell. Fig. 4 shows the transmission spectrum of ZnX for different number of dielectric rods ($N=5, 10$ and 15). The spectrum displays different band gaps which are in the range of $(0.340-0.436) \omega a/2\pi c$ for ZnS, $(0.316-0.429) \omega a/2\pi c$ for ZnSe and $(0.288-0.422) \omega a/2\pi c$ for ZnTe. The band gap has been effectively broadened with the increase of the number of dielectric rods and also with the increase of dielectric constants from ZnS to ZnTe. The calculated spectrum shows complete suppression of transmission in the region precisely coincident with the gap in the band structure, clearly demonstrating the effect of photonic bands on the luminescent properties of ZnX.

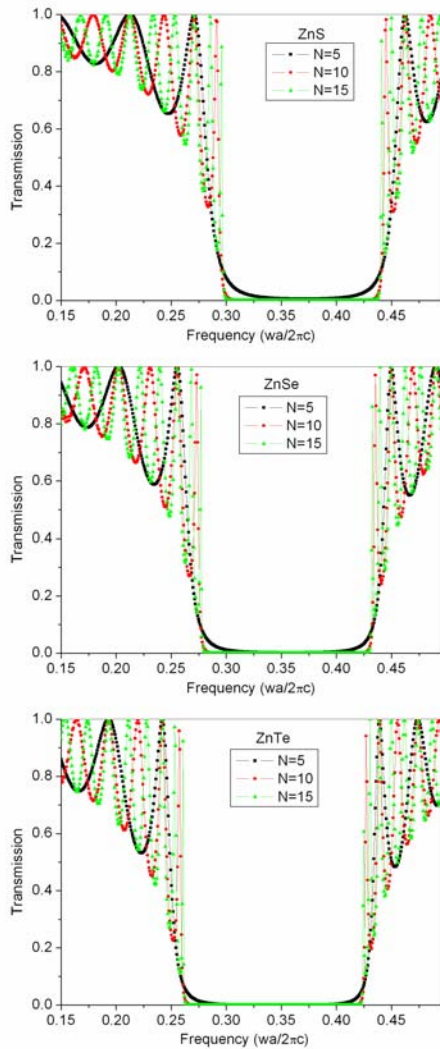


Fig. 4. Transmission spectra of ZnX calculated for a normal-incident planewave through a 2D photonic crystal. Each spectrum shows how the transmission changes when the number of rods (N) are changed.

B. Line Defect 1

In this section, we investigate how the existence of line defects affects the dispersion relation. Line defects could exist if a single row of dielectric rods, removed from the crystal, will break the periodicity in one direction [1,21]. Fig. 5 shows the dispersion diagram of TM polarized photonic crystal wave guide is made by removing a single row in the (10) direction of the crystal shown in the insets of Fig. 5. The diagram is plotted normalized frequency versus normalized wave vector. We observed a single guided mode inside the band gap. The gap is centered at frequencies of $0.368 \omega a/2\pi c$, $0.378 \omega a/2\pi c$, and $0.385 \omega a/2\pi c$ for ZnSe, ZnS and ZnTe respectively. Central frequency of the guided mode has shifted to the higher values from ZnSe to ZnTe. Finally, by changing the geometry of the defect, the cavity properties can be changed, enabling control over the emission color and luminescence properties for ZnX.

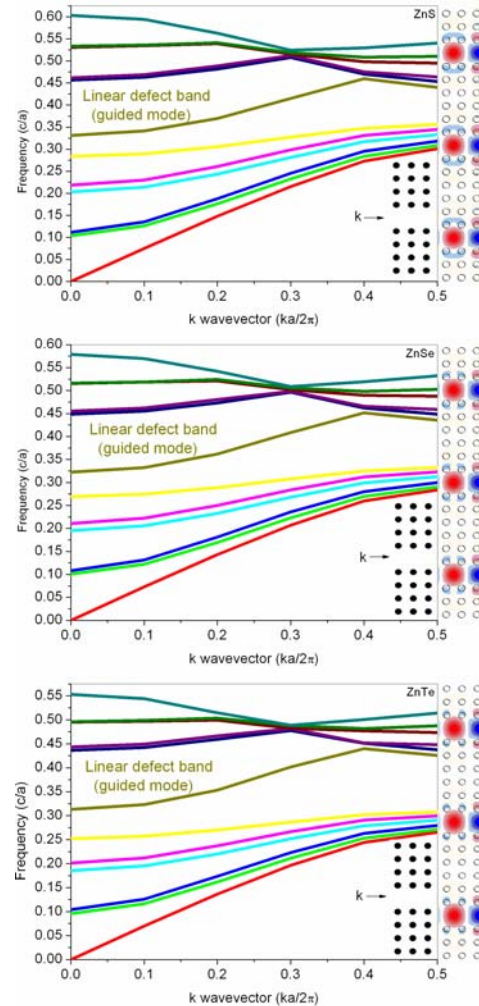


Fig. 5. Left: Band structure of TM modes for a line-defect waveguide in a 2D square lattice of dielectric rods formed by a row of missing rods along the x direction. Right: Electric field E_z of guided mode. This structure supports a single guided band within the band gap.

C. Line Defect 2

Fig. 1 shows the top view of a 2D PhC produced by removing two vertical and horizontal lines of rods from a square-lattice PhC rods-in-air structure. The lattice constant of PhC is a . The time domain simulations were designed as follows: a point source was positioned in the left channel at $(-8, 0)$, and emitted light uniformly in the x - y plane. It sent a TM Gaussian pulse with a center frequency of $0.35c/a$ and a pulse width of $20a/c$. Four detectors with length $2a$ were vertically positioned at four channels. The centers of four detectors are $(-7, 0)$ for left detector, $(7, 0)$ for right detector, $(0, -7)$ for upper detector and $(0, 7)$ for down detector. Each detector accumulates the net energy flow that flowed in the corresponding channel. Each detector is assigned a direction, which designates its direction of positive energy flow. When an energy flow passes through a detector along its direction, this energy flow is considered as positive energy flow. If an energy flow passes through a detector opposite to its direction, this energy flow is considered as negative energy flow. When reflection phenomena exist during the simulations, light passes through a detector from both sides. The directions of the four detectors are positive direction of the x -axis for the left and right detectors, negative direction of the y -axis for the upper detector, and positive direction of the y -axis for the down detector. All detectors are transparent to light, i.e. no influence to propagation of light.

The relation between net energy flow in each channel is shown in Fig. 4, where the y -axis is the ratio of the net energy flow in channels after unification with incident energy to the left channel, which, in fact, is the positive energy flow of the left detector. In Fig. 4, the ratio of net energy flow of the upper channel follows that of the left channel. Much of the incident light along the left channel goes into the upper channel. Less of the incident light enters the upper channel. Indeed, much of the incident light from the left channel is reflected back into the left channel under such case. This similarity of the net energy flow ratio in both left channel and upper channel indicates the control effect of this 2D rods-in-air PhC structure on the incident light from the left channel. The ratio of energy flow distributed among channels is 65% for the left channel, 40% for the right channel, 20% for the upper channel, and 20% for the down channel for ZnS. The ratio of energy flow distributed among channels is 60% for the left channel, 30.0% for the right channel, 15% for the upper channel, and 15% for the down channel for ZnSe. The ratio of energy flow distributed among channels is 27% for the left channel, 12% for the right channel, 10% for the upper channel, and 10% for the down channel for ZnTe. This investigation show that this structure could be practical in the field of integrating optical circuit and light emitting devices.

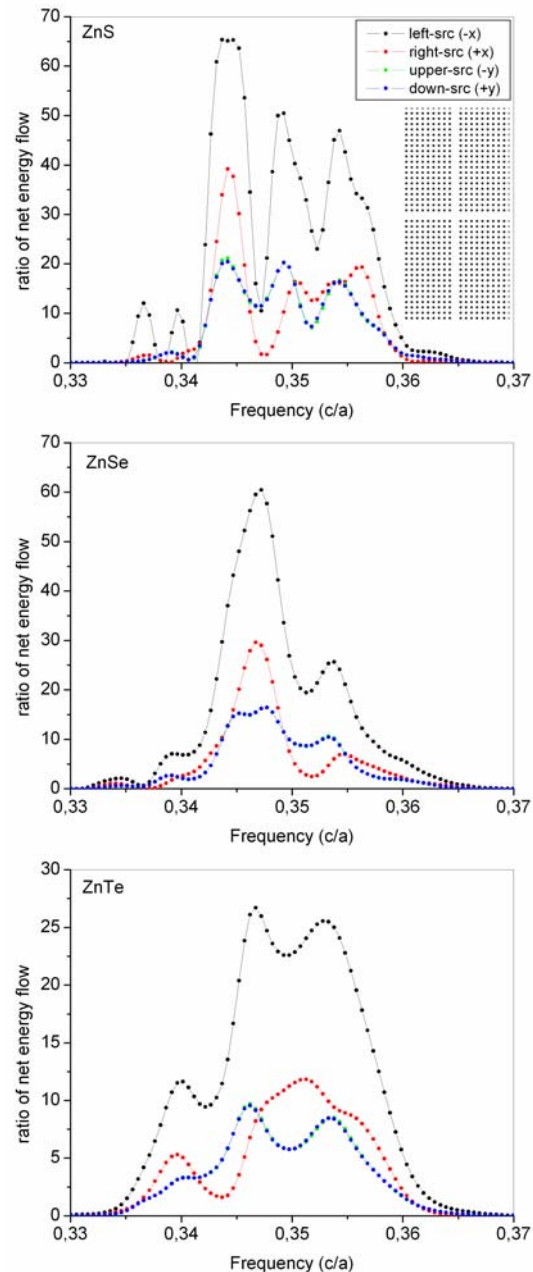


Fig. 6. Top view of 2D rods-in-air square-lattice PhC. Note that x -axis is toward the left, y -axis down, and z -axis vertical to paper pointing away from readers. The origin is located at the center of cross-area, as indicated. Curve represents relation between the ratio of net energy flow in each channel.

4. Conclusion

In conclusion, the photonic band structures of the two-dimensional square lattice of the zinc-blende ZnX ($X = S, Se, Te$) PCs consisting of dielectric rods immersed in air were studied. The calculated results show that a large PBG

can be produced in square lattice by using cylindrical rods. We have outlined basic properties of band gap guiding PCs and have discussed according to three ZnX lattices. Larger band gaps were found for ZnTe. These simulated results should be useful in the design of 2D ZnX based PCs when a large PBG is desired. The wave guiding materials are becoming standard components in future optical systems and any improvements in their properties may be of significant importance. Furthermore, they have high bandgaps and thus are highly transparent in the visible range, which is very important for any application in this spectral region. Due to the photonic band gap effect, the luminescence of a ZnX rod can be suppressed or enhanced. The controllable luminescence of ZnX rods can be useful in the implementation of efficient ZnX rod light emitting devices.

References

- [1] J. D. Joannopoulos, R. D. Meade, J. N. Winn, Photonic Crystals: Molding the Flow of Light, Princeton University Press. (1995).
- [2] E. Yablonovitch, Phys. Rev. Lett., **58**, 2059 (1987).
- [3] S. John, Phys. Rev. Lett. **58**, 2486 (1987).
- [4] K. Sakoda, Optical properties of Photonic Crystals 2nd edn. Springer (2001).
- [5] S. Fan, J. N. Winn, A. Devenyi, J. C. Chen, R. D. Meade, J. D. Joannopoulos, J. Opt. Soc. Am. B., **12**, 1267 (1995).
- [6] S. Li, Y. Y. Lu, J. Lightw. Technol., **28**, 978 (2010).
- [7] W. Park, J. S. King, C. W. Neff, C. Liddell, C. J. Summers, Phys. Stat. Sol. B, **229**, 949 (2002).
- [8] A. H. Reshak, S. Auluck, Physica B **388**, 34 (2007).
- [9] C. S. Kim, M. Kim, D. C. Larrabee, I. Vurgaftman, J. R. Meyer, S. H. Lee, Z. H. Kafafi, J. Appl. Phys. **106**, 113105 (2009).
- [10] A. Bechiri, F. Benmakhlouf, N. Bouarissa, Physics Procedia **2**, 803 (2009).
- [11] J. L. Bredin, Science, **263**, 487 (1994).
- [12] Handbook of Optical Constants of Solids I, Edited by E. D. Palik, Academic, New York (1985).
- [13] Handbook of Optical Constants of Solids II, Edited by E. D. Palik, Academic, New York (1991).
- [14] Taflove A and Hagness S C 2000 Computational Electrodynamics: The Finite-Difference Time-Domain Method 2nd edn (Boston, MA: Artech House Publishers).
- [15] S. G. Johnson, J. D. Joannopoulos, The MIT Photonic-Bands Package (<http://ab-initio.mit.edu/mpb/>).
- [16] K. Busch, G. Von Freymann, S. Linden, S. F. Mingaleev, L. Tkeshelasvili, M. Wegener, Phys. Reports **444**, 101 (2007).
- [17] Z. Zhang, S. Satpathy, Phys. Rev. Lett. **65**, 2650 (1990).
- [18] S. G. Johnson, J. D. Joannopoulos, Opt. Express, **8**, 173 (2001).
- [19] A. F. Oskooi, D. Roundy, M. Ibanescu, P. Bermel, J. D. Joannopoulos, S. G. Johnson, Comp. Phys. Commun. **181**, 687 (2010).
- [20] S. G. Johnson, J. D. Joannopoulos, The MIT Electromagnetic Equation Propagation-Bands Package (<http://ab-initio.mit.edu/meep/>).
- [21] Y. Zhang, H. Lei, B. Li, Optics Communications **283**, 2140 (2010).

*Corresponding author: ufuktepe@gmail.com